

Label Free Fluorometric Characterization of DNA Interaction with Cholate Capped Gold Nanoparticles Using Ethidium Bromide as a Fluorescent Probe

Gunasekaran Dharanivasan · Denison Michael Immanuel Jesse ·
Shanmugam Chandirasekar · Nagappan Rajendiran · Krishnan Kathiravan

Received: 15 March 2014 / Accepted: 2 June 2014 / Published online: 20 June 2014
© Springer Science+Business Media New York 2014

Abstract We demonstrated label free ethidium bromide assisted characterization of DNA interaction with cholate capped AuNPs. Interactions between ss/ds DNA and AuNPs with two different lengths (0.5 and 0.85 kb) were analyzed through fluorescence spectrophotometer and agrose gel electrophoresis analysis. Further results were confirmed by UV–globally visible spectrophotometer, DLS and TEM. As 0.5 and 0.85 kb of ssDNA effectively interacted with AuNPs through the van der Waals interaction which consequently led to the prevention of salt induced aggregation, EtBr intercalations as well as fluorescence shift with less binding constant 0.098 and 0.108 μM , respectively. On the contrary, the same length of dsDNA (0.5 and 0.85 kb) not interacted with AuNPs which led to the NPs aggregation, EtBr intercalation as well as fluorescence shift with increased binding constant 0.166 and 0.599 μM , respectively. This approach helped to understand the mode of interactions of DNA with cholate capped AuNPs without any modifications in a simple method and the results could be readout through the naked eye under the UV transilluminator.

Keywords Gold nanoparticles · ssDNA/dsDNA · EtBr · Fluorescence

G. Dharanivasan · D. M. I. Jesse · K. Kathiravan (✉)
Department of Biotechnology, University of Madras,
Guindy Campus, Chennai 600 025, Tamil Nadu, India
e-mail: kathir68@rediffmail.com

K. Kathiravan
e-mail: drkkathiravan@gmail.com

S. Chandirasekar · N. Rajendiran
Department of Polymer Science, University of Madras, Guindy
Campus, Chennai 600 025, Tamil Nadu, India

Introduction

Nucleic acid based detection of genetic diseases, food pathogens, forensic and environmental samples were considered as the most important in the era of molecular diagnosis [1]. In the last two decades, applications of nanotechnology in the field of diagnosis were explored through the labeling of nanoparticles (NPs) with biological molecules to detect the target substance or molecules rapidly with more sensitivity and flexibility [2]. The use of metal NPs assisted colorimetric methods is very attractive since the process enables rapid visual detection on the spot without any sophisticated equipments [3–6]. Noble metal NPs, especially gold nanoparticles (AuNPs) have been developed as a new family of biosensors for the colorimetric detection of DNA since they exhibit vibrant optical absorbance, high dispersibility in aqueous medium, chemical inertness and biocompatibility [7–9]. AuNPs are used in the detection of single nucleotide polymorphisms (SNPs), single base substitution/mismatch and deletion or insertion [3,9–11]. Thiol-labeled primers and unmodified AuNPs were used to detect target nucleotide sequence in PCR products [12]. AuNPs conjugated ssDNA probes were used in the detection of target DNA sequences and differentiation of *Mycobacterium tuberculosis* [13–15]. Alternatively, the detection of DNA in a single step based on the dispersibility and aggregation of AuNPs probe was achieved using dynamic light scattering (DLS) [16]. However, the preparation of AuNPs conjugated probes (synthesis and functionalization) is laborious, complicated, expensive and time-consuming process [17], the colorimetric detection of target DNA sequence and SNPs using label free unmodified AuNPs with probe based on their electrostatic properties was demonstrated [18–20].

In the earlier studies, the colorimetric detection of target DNA was demonstrated using custom synthesized short oligomer probes and its complementary DNA with citrate capped AuNPs

[3,8–11,18–20]. The effects of different lengths of ssDNA (5, 8, 10, 15, 25, 50 mer) on their interactions with citrate capped AuNPs surface against salt-induced aggregation have been demonstrated recently [21]. Recently, colorimetric detection of geminiviral DNA was demonstrated using degenerate probes and unmodified cholate capped AuNPs. The stability of cholate capped AuNPs was found to be higher than the citrate capped AuNPs in the presence of high salt environment [22]. However, the mode of DNA interactions with cholate capped AuNPs and impact of charges of DNA on the particles aggregation has not been clearly revealed so far. EtBr have been used to stain and visualize both the single strand (ss) and double strand (ds) DNA in agarose gel electrophoresis under the UV transilluminator. Staining occurred through the intercalation of EtBr between the DNA bases via weak interactions (hydrogen bonds and van der Waals interactions) [23–25]. It also involves in the on spot quantification of exponential amplification of DNA in polymerase chain reaction (PCR) [26,27]. In continuation of our previous study [22], herein we investigated the mode of interactions of DNA (0.5 kb and 0.85 kb) with cholate capped AuNPs using ethidium bromide as a fluorescence probe without any modification and labeling.

Materials and Methods

Materials

Hydrogen tetrachloroaurate trihydrate ($\text{HAuCl}_4 \cdot 3\text{H}_2\text{O}$), potassium nitrate (KNO_3), potassium bromide (KBr) and sodium cholate (NaC) were obtained from Sigma-Aldrich and used without further purification. Disodium hydrogen phosphate (Na_2HPO_4), monosodium dihydrogen phosphate (NaH_2PO_4), ethidium bromide (EtBr) and sodium chloride (NaCl) were obtained from Loba-Chemie Ltd., India. Ethylene diamine tetraacetic acid (EDTA) and Agarose were purchased from HiMedia Laboratories Pvt. Ltd. (Mumbai, India). The primers encoding coat protein (CP) gene (ToLCVFP/ToLCVRP), and Rep gene (KKToLCVFP/KKToLCVRP) were designed and synthesized commercially (Eurofins MWG Operon, India Pvt. Ltd., Bangalore, India). Red dye PCR Master Mix was purchased from Ampliqon A/S (Denmark, Germany). PCR was performed in L1996GGD Peltier Model Thermocycler purchased from Lark Innovative Fine Teknowledge, Pvt. Ltd. (India).

Preparation of Cholate Capped AuNPs

Colloidal cholate capped AuNPs were synthesized as described earlier [22]. Briefly, stock solutions of 1.0×10^{-3} M HAuCl_4 and 0.1 M NaC were prepared using deionized double distilled water. For all experiments, the reaction mixture was adjusted to pH 7.0. At optimized reaction conditions, 1 mL of HAuCl_4 solution was added to 0.033 M concentrations of NaC and the final volume

was adjusted to 5 mL using deionized double distilled water. Formation of AuNPs was observed by a change in solution color from light yellow to red. The particles were characterized by UV–visible spectra over the range of 200–1,100 nm was measured with using a Shimadzu UV-1,600 spectrophotometer. TEM analysis was carried out using High Resolution Transmission Electron Microscopy [HR-TEM model Fei Technai G² F30 S-TWIN with 200 kV high-resolution (UHR) pole piece]. Hydrodynamic diameter of particle size was measured by DLS technique using Nanotracs NPA253 (Microtrac, USA).

Primers Design and Synthesis

DNA-A component nucleotide sequences of ToLCV were retrieved from NCBI and aligned by multiple sequences alignment tools using BioEdit version 7.0.5.3 software. Based on this alignment, ToLCV specific degenerate primers were designed and custom synthesized to amplify CP (0.5 kb) and Rep (0.85 kb) genes (Table 1).

Amplification of Begomoviral DNA

The total DNA was extracted from begomovirus infected Tomato leaf samples and it was confirmed by 0.8 w/v% agarose gel electrophoresis. ToLCV CP and Rep genes were amplified in 0.5 kb and 0.85 kb in length respectively by PCR. The reaction mixture was prepared to the total reaction volume of 50 μL by the addition 25 μL of $2\times$ red dye PCR Master Mix, 22.5 μL DNase/RNase free deionized water, virus specific primers (100 pmol of 0.625 μL Forward Primer and 0.625 μL Reverse Primer) and template DNA (1.25 μL) of this virus were added separately to CP and Rep genes marked tubes. The amplification programmes consist the following steps which are the initial denaturation at 94°C for 5 min followed by denaturation at 94°C for 1 min, annealing at 60°C for CP gene (ToLCVFP/ToLCVRP) and 53.2°C for Rep gene (KKToLCVFP/KKToLCVRP) for 1 min, extension at 72°C for 2 min with 25 cycles and a final extension at 72°C for 5 min.

Elution of Amplified DNA

Amplified PCR products were eluted from the reaction mixture by addition of 5 μL of sodium acetate solution (pH 4.2) and 100 μL of 95 % ethanol to 50 μL of reaction volume in PCR tube. The mixture was vortexed gently and incubated at -20°C for 40 min. Then the mixture was centrifuged at 10,000 rpm for 20 min. The supernatant was discarded carefully and pellet was washed with 70 v/v % ethanol. After washing, the pellet was air dried at RT and suspended in 50 μL RNase/DNase free deionized water for further studies. Eluted products were electrophoresed in 1.2 w/v % agarose, visualized under the UV transilluminator and quantified using Nanodrop 2000c Spectrophotometer, Thermo scientific Inc. (USA).

Table 1 Custom synthesized primer sequences specific for CP and Rep genes of ToLCV

Length of DNA	Name of Virus	Sequence ID	Primer Sequences ^a
0.5 kb	Tomato leaf curl Virus	ToLCVFP	5'- GAATTCATGTCSAAGCGWCCRCGAGA-3'
		ToLCVRP	5'- GGTACCATTCTTMACAGTWGCAGTGC-3'
0.85 kb	Tomato leaf curl Virus	KKToLCVFP	5'- ATGAAGTAWGAACAGCCRCAC - 3'
		KKToLCVRP	5'- CCATCCGAACATTTCAGGGAG - 3'

S- G or C; M- A or C; W- A or T; R- A or G

^a Underlined colored letters in the primers sequences represent the degenerate bases

Fluorescence Studies

Single standard DNA was prepared by heat denaturation of dsDNA at 95°C for 5 min and it was used immediately before renaturation in these studies. The samples 0.5 kb and 0.85 kb length of ssDNA and dsDNA were incubated with AuNPs for 1 h at RT. After incubation, samples were loaded in 1.2 w/v % of agarose gel containing the EtBr (0.5 mg/mL) and allowed to run at 50 mV until the red color band moved three fourth of distance. Then the gel was observed under the white light and UV light. The images were captured to analyze the EtBr intercalation. In the fluorescence study, 3 mL of each samples (EtBr, AuNPs+EtBr, 0.5 kb and 0.85 kb length of ssDNA with AuNPs+EtBr, 0.5 kb and 0.85 kb length of dsDNA with AuNPs+EtBr, and DNA+Br) (Table 2) containing EtBr (0.5 mg/mL) were analyzed using 1 cm quartz cuvettes. The fluorescence was recorded from 400 to 800 nm by exciting at 285 nm using Cary Eclipse (EL07023695) fluorescence spectrophotometer and image was captured under the UV transilluminator (UV light at 310 nm). The binding parameters of EtBr with 0.5 kb and 0.85 kb ss/dsDNA in the presence of AuNPs were determined from the fluorescence spectra using the Scatchard equation ($r/C_f = K_b$; K_b - binding constant) at a constant molar concentration of EtBr, AuNPs and DNA in different length (0.5 kb and 0.85 kb) and different state (ssDNA and dsDNA) [28].

UV–Visible Spectrophotometer Analysis

The stability of cholate capped AuNPs analyzed through the salt induced aggregation using NaCl at different concentrations (1–

6 M). The salt concentration was optimized using different volumes of 6 M NaCl (10–50 μL) in the presence of 50 μL of 10 mM sodium phosphate buffer [8] and 400 μL of cholate capped AuNPs. The solution was mixed well and kept at room temperature for 10 min and subsequently absorbance spectra were taken and the concentration was optimized as 50 μL of 6 M NaCl. The interaction properties of ssDNA (0.5–0.85 kb length) with AuNPs were analyzed by adding different concentrations of ssDNA (25 nM, 50 nM, 75 nM, 100 nM and 125 nM) to 400 μL AuNPs and their stability were measured by keeping the mixture at RT for 1 h. After incubation, 50 μL of 6 M NaCl was added and left at RT for 10 min. The change in the colour of the solution was measured by using UV–visible spectrophotometer.

DLS and HR-TEM Analysis

Hydrodynamic diameter of synthesized AuNPs was measured in the presence of optimized volume of ssDNA/dsDNA by DLS. 3 mL of samples containing optimized concentration of ssDNA and dsDNA (0.5 kb and 0.85 kb) with phosphate buffer and AuNPs were kept for 1 h at RT. Followed by, 300 μL of NaCl was added and incubated for 10 min at RT. After incubation, the solution was kept in dust-free light scattering cell and analyzed with analysis time of 300 sec. The size of dispersed and aggregated AuNPs with different lengths of ssDNA and dsDNA were measured using the HR-TEM. About 1–2 μL of the samples were added to the carbon coated copper grid and kept for drying at RT. The size of AuNPs with ss/dsDNA was analyzed at 200 kV.

Table 2 Composition matrix used in fluorescence study

Samples	EtBr (μL)	Buffer (μL)	ssDNA (μL)	dsDNA (μL)	AuNPs (μL)	Water (μL)
(a) EtBr			-	-	-	2,850
(b) EtBr+DNA			-	150	-	2,700
(c) EtBr+AuNPs			-	-	2,500	350
(d) EtBr+0.5 kb ssDNA+AuNPs			150 (0.5 kb)	-	2,500	350
(e) EtBr+0.5 kb dsDNA+AuNPs	0.3	150	-	150 (0.5 kb)	2,500	350
(f) EtBr+0.85 kb ssDNA+AuNPs			150 (0.85 kb)	-	2,500	350
(g) EtBr+0.5 kb dsDNA+AuNPs			-	150 (0.85 kb)	2,500	350

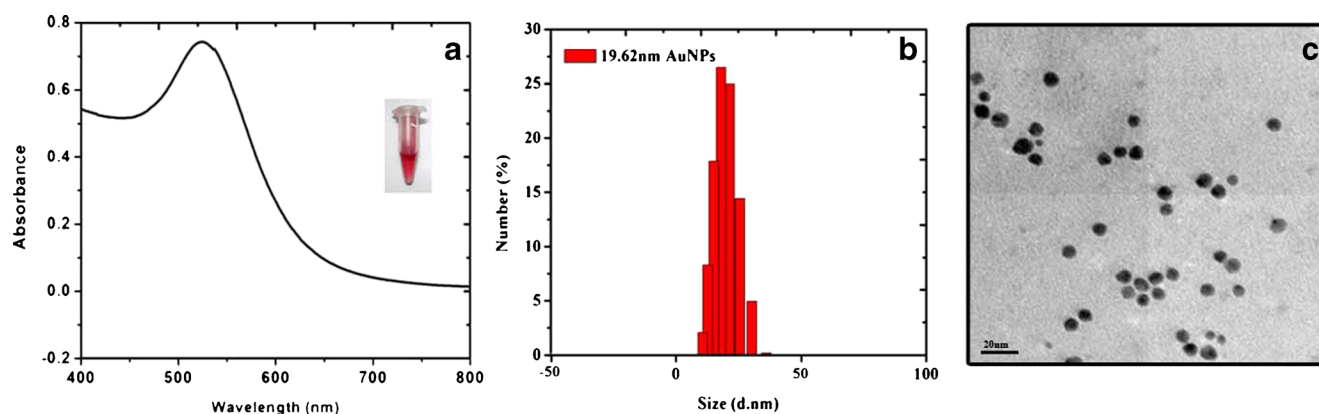


Fig. 1 **a** - UV-visible absorbance spectra of cholate capped AuNP showing SPR band at 526 nm. Inset photograph shows synthesized AuNPs in red color. **b** - Hydrodynamic diameter size and distribution of AuNPs in nm, **c** - TEM image showing spherical shaped AuNPs (~12 nm size)

Results and Discussion

Synthesis of Cholate Encapsulated AuNPs and PCR Amplification of DNA

Cholate encapsulated AuNPs were synthesized at RT based on the early described method [22]. The yellow color of the solution was changed to red color which indicates the formation of AuNPs (Fig. 1a, inset image) and the corresponding UV-visible absorption spectra shows sharp surface plasmon resonance (SPR) band at 526 nm (Fig. 1a). The average hydrodynamic diameter of synthesized AuNPs measured by DLS was found to be ~19.62 nm (Fig. 1b). HR-TEM analysis

shows spherical shape AuNPs with the size ~12 nm in diameter (Fig. 1c). The formation AuNPs by the reduction of Au^{3+} ion to Au^0 metal by accepting electrons from sodium cholate and it also stabilize the particle from the continuous nucleation growth. Therefore, sodium cholate acting as reducing as well as capping agent in this method [22].

The stability of cholate capped AuNPs was analyzed through the salt induced aggregation. The aggregation of AuNPs was found to be increased while increasing the concentration of NaCl from 1 to 6 M. The complete aggregation of AuNPs was found at 6 M NaCl (data not shown). 0.5 and 0.85 kb length of ssDNA and dsDNA were obtained by PCR amplification of Tomato leaf Curl Viral (ToLCV) DNA using specific degenerate primers [29]. Fig. 2 agarose gel image shows PCR amplified 0.5 kb and 0.85 kb ToLCV DNA in lane 1 and 2, respectively and were eluted and quantified by spectrophotometrically. It were found to be 192.1 $\text{ng}/\mu\text{L}$ and 189.8 $\text{ng}/\mu\text{L}$ for 0.5 kb and 0.85 kb DNA, respectively. The synthesized AuNPs and amplified DNA were used for further study.

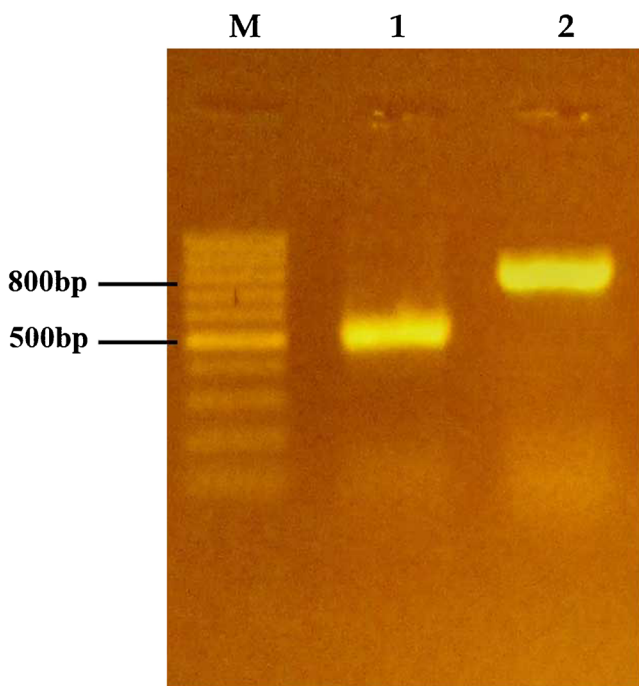
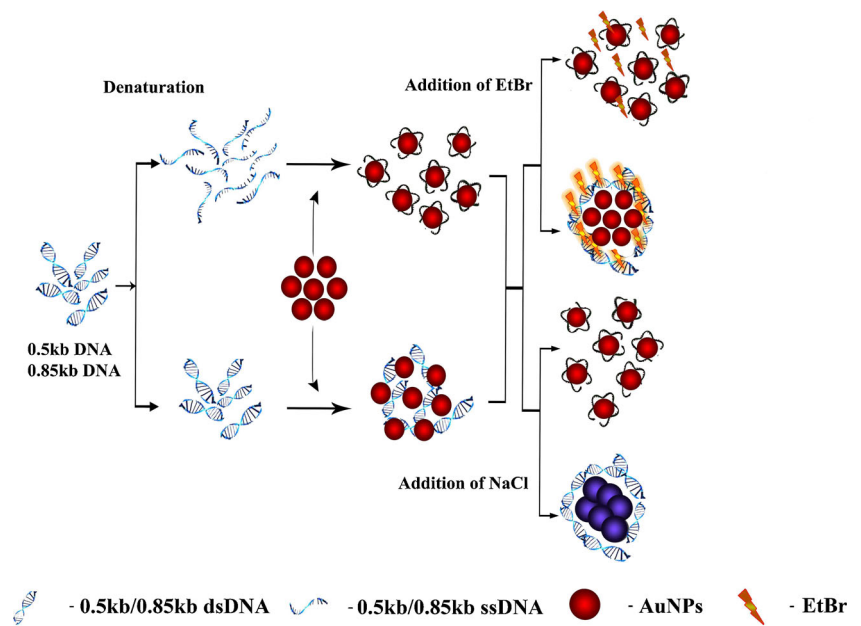


Fig. 2 Agarose gel image showing PCR amplified products of 0.5 kb and 0.85 kb length DNA from ToLCV, Lane M - 100 bp DNA ladder, lane 1- 0.5 kb length DNA and lane 2- 0.85 kb length DNA

EtBr Fluorescence Study for Interaction of DNA with AuNPs

The mode of interaction of ss/dsDNA on the AuNPs was investigated using EtBr (DNA intercalator) as a fluorescent probe (scheme-globally 1). The intercalation of EtBr with nucleic acid (ss/dsDNA) occurs at every 2.5 bp in perpendicular manner through the stacking forces such as van der Waals and hydrogen bond interactions [28,30–33]. Li and Rothberg hypothetically described the mode of interactions of DNA with AuNPs using fluorescent tag probe based on the quenching of fluorescence by AuNPs [18,19]. Liu discussed the mechanism of adsorption of DNA with citrate capped AuNPs in his critical review [34]. The interaction of negatively charged dsDNA with positively charged AuNPs was characterized using EtBr as fluorescent probe [33]. Since the

Scheme 1 Fluorometric characterization of ss/dsDNA interaction (0.5 and 0.85 kb) with cholate capped gold nanoparticles using EtBr



interaction of both EtBr and AuNPs with DNA are similar [28,30–33], we hypothesize that the EtBr intercalation property can be used to investigate the mode of interaction of DNA with AuNPs. A clear red color band of both ssDNA-AuNPs and dsDNA-AuNPs was found in the agarose gel when visualized through naked eye (Fig. 3a). However the same gel was visualized under UV transilluminator, a clear red-orange band was observed only in the 0.5 and 0.85 kb length dsDNA with AuNPs and not in the ssDNA-AuNPs (Fig. 3b). This clearly indicates that the EtBr intercalates only with dsDNA with AuNPs, which exhibit fluorescence but not with ssDNA-AuNPs. This is because the nitrogenous bases of ssDNA get covered on AuNPs through van der Waals interaction to form

ssDNA-AuNPs complex that leads to prevent the formation of self coiled secondary structure for the EtBr intercalation.

Fluorescence spectroscopy was used for further investigation of our hypothesis about the interaction properties of different lengths of ss/dsDNA (0.5 and 0.85 kb length) on the AuNPs surface using EtBr. The fluorescence emission spectra of free EtBr in aqueous solution showed maxima at 620 nm (Fig. 4 curve ‘a’). After the addition of dsDNA the emission maxima of probe was shifted to 600 nm with decreased intensity and subsequently a new peak appeared at 566 nm along with significant intensity (Fig. 4 curve b). This could be due to intercalation of the EtBr with dsDNA that leads to fluorescence shift from red to reddish orange.

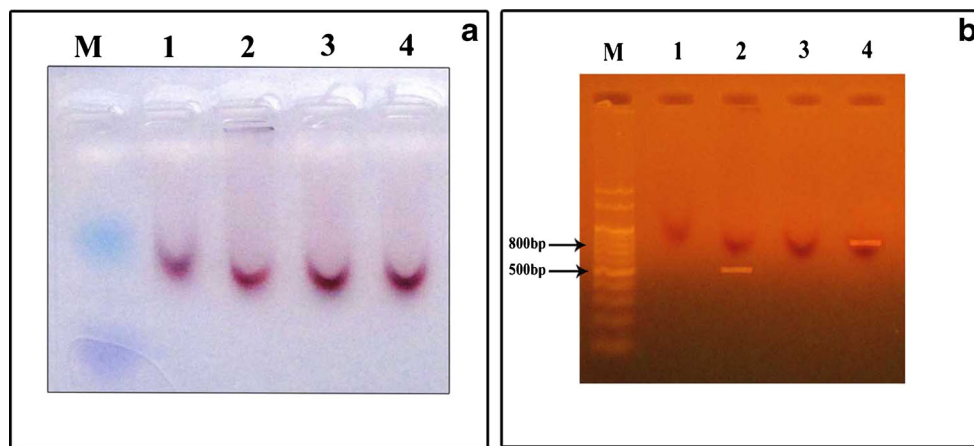
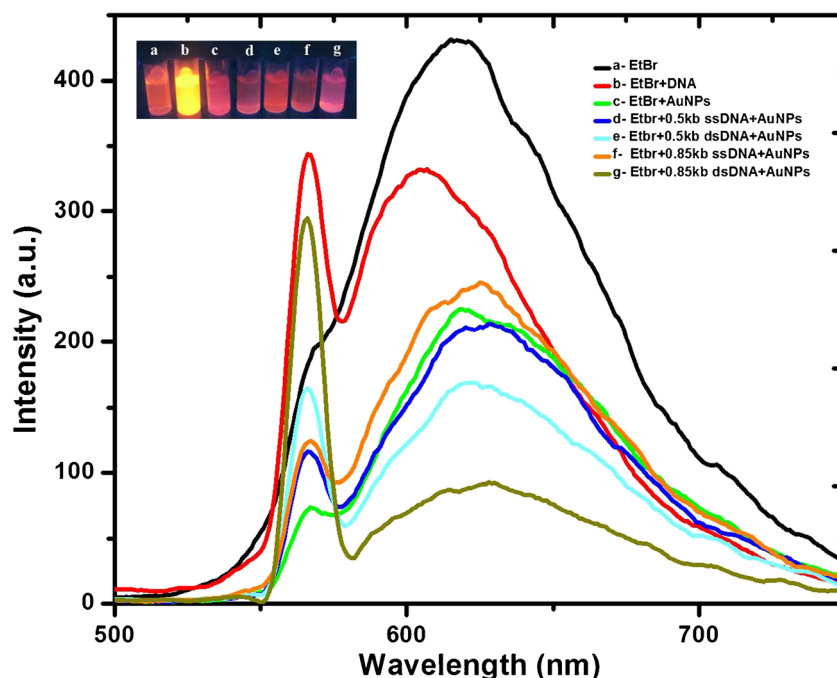


Fig. 3 Agarose gel electrophoresis with the ssDNA/dsDNA stabilized and destabilized AuNPs. a - 1.2 w/v % agarose gel under the white light. lane M – 100 bp ladder, lane 1–0.5 kb length ssDNA stabilized AuNPs, lane 2–0.5 kb length dsDNA destabilized AuNPs, lane 3–0.85 kb length ssDNA stabilized AuNPs and lane 4–0.85 kb length dsDNA destabilized

AuNPs. b- agarose gel visualized under the UV light after the EtBr staining. Lanes 1 & 3 - without DNA band indicating that ssDNA covered on the AuNPs not intercalating with EtBr and Lanes 2 & 4 - with DNA bands indicating dsDNA intercalated with EtBr and not interacting with AuNPs.

Fig. 4 Fluorescence emission spectra. **a** EtBr (high intensity peak at 620 nm), **b** EtBr+DNA, **c** EtBr+AuNPs, **d** EtBr+0.5 kb length ssDNA+AuNPs, **e** EtBr+0.5 kb length dsDNA+AuNPs, **f** EtBr+0.85 kb length ssDNA+AuNPs and **g** EtBr+0.85 kb length dsDNA+AuNPs. Inset photographic image (**a–g**) shows corresponding fluorescence of the solutions under the UV-transilluminator



Addition of AuNPs to EtBr resulted in decrease in the intensity of emission peak indicating that the probe molecules were quenched by the AuNPs (~50 %) (Fig. 4 curve c) [32,33]. However, in the presence of two different lengths of ssDNA (0.5 and 0.85 kb) stabilized AuNPs, a maximum intensity of probe peak was seen at 620 nm along with a small peak at 566 nm (Fig. 4 curve d and e, respectively). This could be due to the strong interaction of ssDNA on the AuNPs through the van der Waals force which prevents the formation of self coiled secondary structure for the intercalation of EtBr at maximum level and the presence small peak at 566 nm could be due to the presence of small number of unbounded self coiled ssDNA. The intercalation of EtBr with different length of dsDNA was observed by a decrease in the intensity of EtBr peak at 620 nm and an enhanced peak at 566 nm (Fig. 4 curve f and g respectively). This could be due to the absence of interaction of dsDNA with AuNPs, which was confirmed by

EtBr intercalation and fluorescence shift. However, the extent of change in the intensity of peak observed at 566 nm for 0.85 kb was greater [295.06 (a.u.)] than 0.5 kb length dsDNA [164.62 (a.u.)]. It could be due to the difference in the length as well as the number of EtBr molecules intercalated with DNA and fluorescence shift [~ 340 EtBr molecules/0.85 kb dsDNA and ~ 200 EtBr/0.5 kb dsDNA of 150 μL (100 nM)].

The binding constant of EtBr with 0.5 kb and 0.85 kb ss/dsDNA in the presence of AuNPs also summarized in Table 3. The binding constant of EtBr with ssDNA of 0.5 kb and 0.85 kb was found to be very low than the binding constant of EtBr with dsDNA (0.5 kb and 0.85 kb size) in the presence of AuNPs. This is due to the adsorption of ssDNA on the cholate capped AuNPs which is similar to the adsorption of ssDNA with citrate capped AuNPs [34]. This adsorption might be occur via N6, N7 nitrogen atom of purine bases (A and G), N3 nitrogen atom and C4 keto oxygen of pyrimidine

Table 3 Determination EtBr binding parameters with ssDNA and dsDNA (0.5 kb and 0.85 kb) in the presence of AuNPs

Samples	Intensity (a.u.) at 566 nm	[EtBr] (10^{-4} μM)			r	r/C_f (μM)
		C_0	C_b	C_f		
EtBr+DNA	343.07	3.81	3.08	0.73	0.808	1.107
EtBr+ssDNA (0.5 kb)+AuNPs	115.8		1.04	2.77	0.273	0.098
EtBr+ssDNA (0.85 kb)+AuNPs	124.5		1.12	2.69	0.293	0.108
EtBr+dsDNA (0.5 kb)+AuNPs	164.6		1.48	2.33	0.388	0.166
EtBr+dsDNA (0.85 kb)+AuNPs	295.0		2.65	1.16	0.695	0.599

C_0 - initial concentration of EtBr; C_b - concentration of EtBr bound to DNA; C_f - concentration of the free EtBr; r - proportion between the concentration of EtBr bound to DNA (C_b) and the initial concentration of EtBr (C_0)

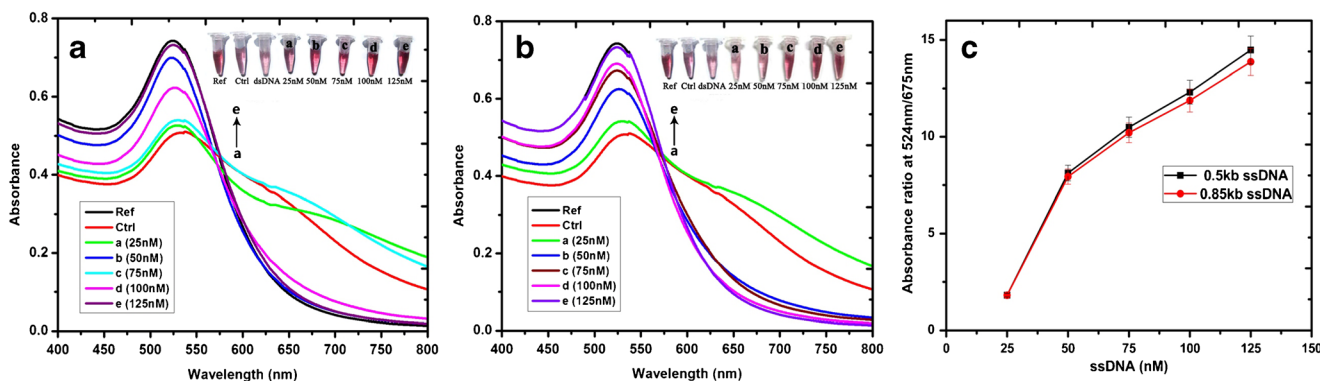


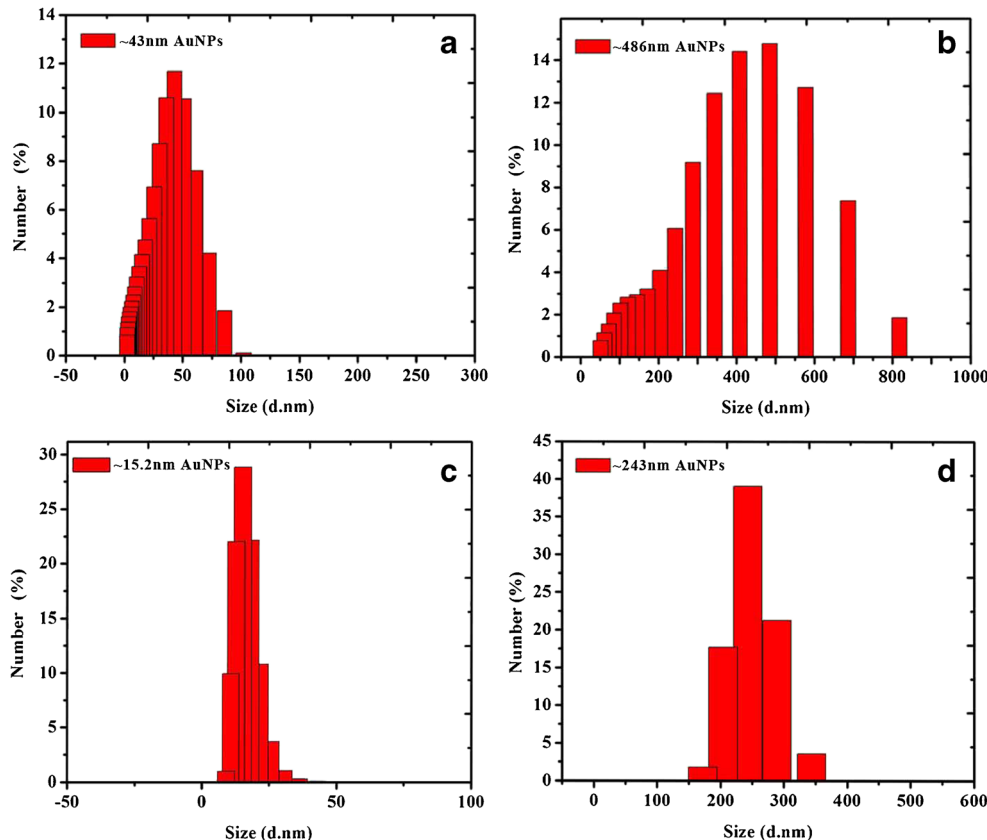
Fig. 5 UV-Vis absorbance spectra of 0.5 kb **a** and 0.85 kb **b** ssDNA stabilized AuNPs. Curves a–e represents different concentrations of 0.5 kb and 0.85 kb length of ssDNA from 25 to 125 nM respectively. The stability of AuNPs was gradually increased while increasing concentration of ssDNA from 25 nM to 125 nM and maximum stability was achieved at 100 nM and 125 nM for 0.5 kb and 0.85 kb length ssDNA respectively. Ref and Ctrl serve as reference and control respectively. DS

denotes dsDNA. The inset photographic images show the corresponding color stability of AuNPs in the presence of salt. **c** Ratio of absorbance (524 nm/675 nm) versus concentrations of ssDNA indicating the stability of AuNPs. Degree of stability of AuNPs with 0.5 kb ssDNA (black line with closed square) and 0.85 kb length ssDNA (red line with closed circles) against salt induced aggregation

bases (C and T) of DNA with C=O of cholate capped AuNPs. This adsorption includes van der Waals force, hydrophobic interaction and induced dipole interactions which prevent the renaturation of ssDNA to form a double helix and self coiled secondary structures favourable for EtBr intercalation. Therefore, EtBr intercalation is very less with ssDNA-AuNPs complex and it was confirmed in the binding constant.

In the case of dsDNA, EtBr intercalation and binding constant were found to be very high in the presence of AuNPs. This is due to the absence of chemisorption of dsDNA with AuNPs and high electronegativity repulsion among dsDNA and AuNPs. As a result dsDNA is free in the solution with rigid double helix structure favourable for the perpendicular intercalation of EtBr through the stacking forces and hydrogen

Fig. 6 Hydrodynamic size distribution of ssDNA and dsDNA with NaC capped AuNPs **a** 0.5 kb length ssDNA stabilized NaC capped AuNPs (~43 nm), **b** 0.5 kb length dsDNA with AuNPs (~486 nm), **c** 0.85 kb length of ssDNA stabilized AuNPs (~15.9 nm) and **d** 0.85 kb length of dsDNA with AuNPs (243 nm)



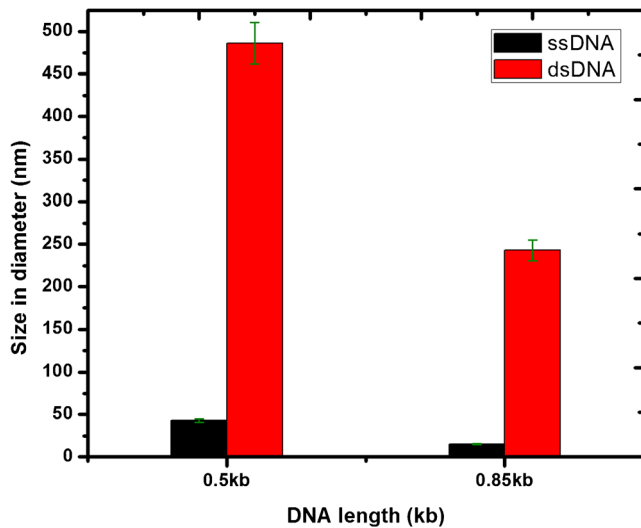
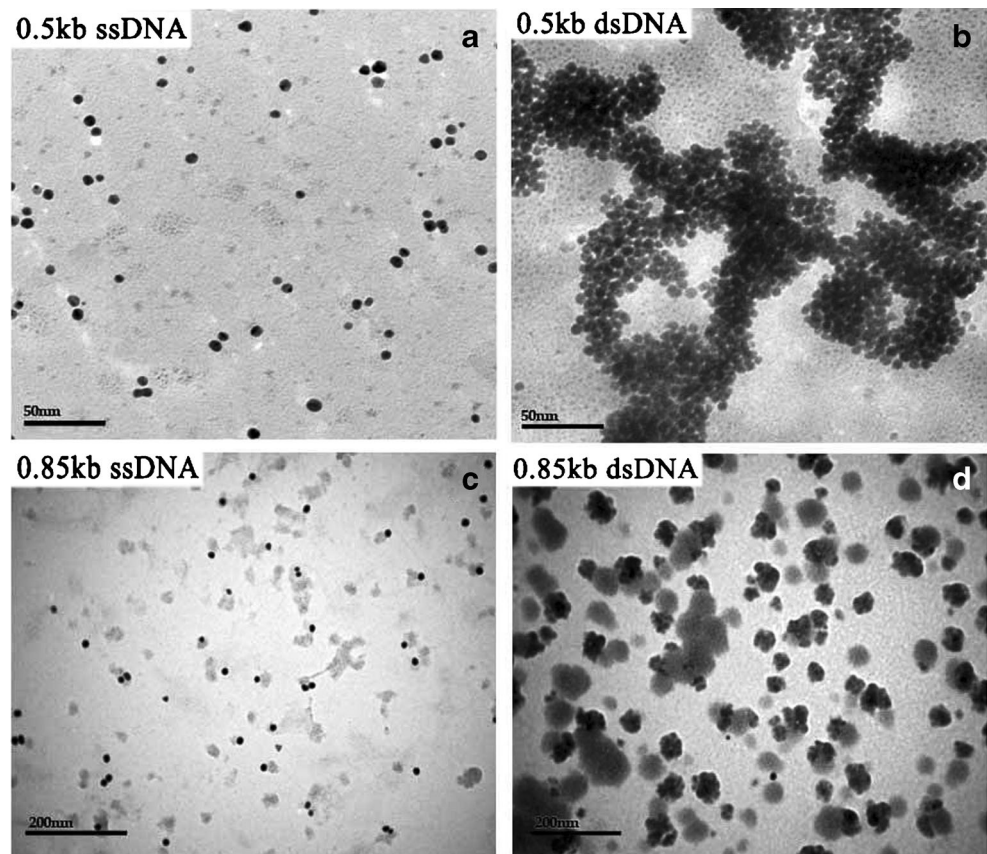


Fig. 7 DLS bar graph for the degree of aggregation and distribution of NaC capped AuNPs with ssDNA and dsDNA. 0.5 and 0.85 kb length ssDNA (*Black bar*) stabilized NaC capped AuNPs ~43 nm and ~15.2 nm respectively, 0.5 and 0.85 kb length dsDNA (*Red bar*) with AuNPs ~486 nm and ~243 nm respectively

bonds. Particularly, EtBr intercalation with 0.85 kb dsDNA was greater than the 0.5 kb dsDNA and this could be due to the differences in the number of bp as well as EtBr interactions between 0.5 kb and 0.85 kb dsDNA [28,32–34].

Fig. 8 TEM images. 0.5 kb **a** and 0.85 kb **c** length ssDNA stabilized AuNPs and 0.5 kb **b** and 0.85 kb **d** length dsDNA with aggregated AuNPs



UV–Visible Spectrophotometer Analysis

The interactions of ss/ds DNA with cholate capped AuNPs were reconfirmed by UV–visible spectrophotometer studies. The characteristic SPR band of aggregated AuNPs ~700 nm gradually decreased and the absorption band at 524 nm gradually increased with increase in ssDNA concentration from 25 to 125 nM (Fig. 5a and b, curve a-e, inset a-e), which confirms that the particles are stabilized in the presence of salt. However no significant change in the absorption intensity of AuNPs was observed at 100 and 125 nM of 0.5 and 0.85 kb ssDNA respectively and the colour of the solution remained constant. The plot of degree of stabilization of ssDNA on AuNPs indicating that 100 nM of 0.5 kb of ssDNA and 125 nM of 0.85 kb of ssDNA enough to stabilize the AuNPs effectively (Fig. 5c). In the presence of dsDNA (0.5 and 0.85 kb), the AuNPs aggregated after the addition of salt. It was indicated by the color change from red to blue that led to decrease in the intensity of the peak at 524 nm along with appearance of new peak in the longer wavelength region (Fig. 5a and b, inset image “dsDNA”, curve “dsDNA” of UV–visible spectra). The rationale is that dsDNA does not adsorb on the AuNP surface due to electrostatic

repulsion between NPs and dsDNA. Similar observations were reported by Li and Rothberg [18–20]. The difference in the degree of stabilization of AuNPs indicates that the 0.5 kb length of ssDNA has high stabilizing capacity than the 0.85 kb of ssDNA, which could be due to the maximum contact point of 0.5 kb of ssDNA on the AuNPs surface than the 0.85 kb. This could be due to the less coiled secondary structure with more flexible and freely exposed nucleobases. Therefore, 0.5 and 0.85 kb length of ssDNA adsorbed strongly and irreversibly on the AuNPs surface through van der Waals interaction occurred between the nucleobases of ssDNA and AuNPs which prevent the aggregation of AuNPs in high salt concentration. Also the exposes of electro negative phosphate back bone on outer surface of ssDNA-AuNPs complex lead to electrostatic repulsion among them. On the other hand dsDNA is unable to interact on the AuNPs surface in the presence of salt. This could be due to the electro-negative repulsion between dsDNA and AuNPs.

DLS and HRTEM Analysis

Hydrodynamic diameters of AuNPs interacted with ssDNA and dsDNA were characterized by DLS method (Fig. 6a, b - 0.5 and 0.85 kb ssDNA with AuNPs; c & d 0.5 and 0.85 kb dsDNA with AuNPs respectively). The 0.5 and 0.85 kb length of ssDNA were found to be stabilizing AuNPs in the high salt environment (Fig. 7 Black bar). The average size of 0.5 and 0.85 kb length of ssDNA to stabilize the AuNPs was found to be ~43 and ~15.2 nm and for dsDNA the average hydrodynamic diameter of aggregated AuNPs was increased dramatically to ~486 and ~243 nm, respectively (Fig. 7 Red bar). The huge variations in hydrodynamic diameter of AuNPs with different lengths of ssDNA and dsDNA, indicates that the length and electronegative charges of DNA play an important role on the size of AuNPs in the presence of salt [12,35]. Where, longer length DNA with more electronegative charges is reported to be effectively controlling the degree of aggregation of AuNPs after the addition of salt. This could be due to the increases of electronegative of phosphate backbone in the ssDNA/dsDNA with an increase in the length of the DNA. Similarly variation in the particle size in diameter was confirmed by TEM analysis (Fig. 8). The dispersed AuNPs with an average size 10–12 nm for 0.5 and 0.85 kb length of ssDNA shows that even a large length of ssDNA can stabilize AuNPs against salt induced aggregation (Fig. 8a–c). Contrary to this, only AuNPs aggregation was observed in the presence of 0.5 and 0.85 kb length of dsDNA after the addition of salt (Fig. 8b–d). These results were agreeable with the UV–visible spectrophotometer studies. The degree of stabilization is found to be determined by concentration and length of ssDNA.

Conclusion

In conclusion, we have investigated mode of interaction of ss/dsDNA (0.5 and 0.85 kb) with cholate encapsulated AuNPs using EtBr as fluorescence probe without any conjugation and modification. The mode of interactions of DNA with AuNPs was characterized using EtBr and the results could be visualized by naked eye through UV transilluminator. Long length of ssDNA (0.5 and 0.85 kb) were found to be interacting effectively with AuNPs to stabilize against salt induced aggregation through the van der Waals force and the dsDNA was unable to stabilize the AuNPs. While increasing the length of DNA, stability of AuNPs slightly decreased and effectively controlled the degree of salt induced particles aggregation. It proves that the lengths and charges of DNA play an important role on AuNPs stabilization and aggregation. This EtBr intercalation is simple approach, sensitive, cost effective, less time consuming than the fluorescence tagging studies for the understanding the basic phenomenon between the nanobio interface. It is helpful to understand the mode of interactions of DNA with AuNPs and It proves that the mode of interaction of cholate capped AuNPs was similar with citrate capped AuNPs. Its hope that cholate capped AuNPs can be used as optical sensing element in further development of nanoassay method for the detection of DNA.

Acknowledgments Authors thanks Mr. R. Shanker babu, Department of Polymer science, University of Madras, Chennai for DLS analysis. The authors profusely thank Dr. S. Seshadri, Scientist, Shri AMM Murugappa Chettiar Research Centre, Taramani, Chennai for valuable scientific discussion and suggestions. The authors also thanks to UGC [F. No. 37-440/2009 (SR)] and NCNSNT (F. No. C-2/Res.Pro/NSNT/Proj.No.7/2011/192) for financial supports.

References

1. Tsongalis GJ, Silverman LM (2006) Molecular diagnostics: a historical perspective. *Clin Chim Acta* 369(188):192
2. Jain KK (2003) Nanodiagnostics: application of nanotechnology in molecular diagnostics. *Expert Rev Mol Diagn* 3(153):161
3. Storhoff JJ, Elghanian R, Mucic RC, Mirkin CA, Letsinger RL (1998) One-Pot colorimetric differentiation of polynucleotides with single base imperfections using gold nanoparticle probes. *J Am Chem Soc* 120:1959–1964
4. Niemeyer MC (2001) Nanoparticles, proteins, and nucleic acids: biotechnology meets materials science. *Angew Chem Int Ed* 40(4128):4158
5. Liu J, Lu Y (2006) Preparation of aptamer-linked gold nanoparticle purple aggregates for colorimetric sensing of analytes. *Nat Protoc* 1(246):252
6. Rho S, Kim JS, Lee CS, Chang HJ, Kang H-G, Choi J (2009) Colorimetric detection of ssDNA in a solution. *Curr Appl Phys* 9(534):537
7. Mirkin AC, Letsinger LR, Mucic CR, Storhoff JJ (1996) A DNA based method for rationally assembling nanoparticles into macroscopic materials. *Nature* 382(607):609
8. Sato K, Hosokawa K, Maeda M (2005) Non-cross-linking gold nanoparticle aggregation as a detection method for single-base substitutions. *Nucleic Acids Res* 33(1):5

9. Liz-Marza'n LM (2006) Tailoring surface plasmons through the morphology and assembly of metal nanoparticles. *Langmuir* 22(32):41
10. Doria G, Franco R, Baptista P (2007) Nanodiagnosics: fast colorimetric method for single nucleotide polymorphism/mutation detection. *IET Nanobiotechnol* 1(53):57
11. Qin JW, Yung LYL (2007) Nanoparticle-based detection and quantification of DNA with single nucleotide polymorphism (SNP) discrimination selectivity. *Nucleic Acids Res* 35(1):8
12. Jung LY, Jung C, Parab H, Li T, Park GH (2010) Direct colorimetric diagnosis of pathogen infections by utilizing thiol-labeled PCR primers and unmodified gold nanoparticles. *Biosens Bioelectron* 25:1941–1946
13. Upadhyay P, Hanif M, Bhaskar S (2006) Visual detection of IS6110 of *Mycobacterium tuberculosis* in sputum samples using a test based on colloidal gold and latex beads. *Clin Microbiol Infect* 12(1118):1122
14. Costa P, Amaro A, Botelho V, Inacio J, Baptista PV (2010) Gold nanoprobe assay for the identification of mycobacteria of the *Mycobacterium tuberculosis* complex. *Clin Microbiol Infect* 16(1464):1469
15. Wen Y, McLaughlin KC, Lo KP, Yang H, Sleiman FH (2010) Stable gold nanoparticle conjugation to internal DNA positions: facile generation of discrete gold nanoparticle-DNA assemblies. *Bioconjug Chem* 21(1413):1416
16. Dai Q, Liu X, Coutts J, Austin L, Huo Q (2008) One-step highly sensitive method for DNA detection using dynamic light scattering. *J Am Chem Soc* 130(8138):8139
17. Zhao W, Lin L, Hsing MI (2009) Rapid synthesis of DNA-functionalized gold nanoparticles in salt solution using mononucleotide-mediated conjugation. *Bioconjug Chem* 20(1218):1222
18. Li H, Rothberg L (2004) Colorimetric detection of DNA sequences based on electrostatic interactions with unmodified gold nanoparticles. *Proc Natl Acad Sci* 101(14036):14039
19. Li H, Rothberg L (2004) Label-free colorimetric detection of specific sequences in genomic DNA amplified by the polymerase chain reaction. *J Am Chem Soc* 126(10958):10961
20. Li H, Rothberg L (2005) Label-free colorimetric detection of specific sequences in PCR amplified DNA. *NSTI-Nanotech* 1:472–473
21. Shen Q, Nie Z, Guo M, Zhong C-J, Lin B, Li W, Yao S (2009) Simple and rapid colorimetric sensing of enzymatic cleavage and oxidative damage of single-stranded DNA with unmodified gold nanoparticles as indicator. *Chem Commun* 929:931
22. Chandirasekar S, Dharanivasan G, Kasthuri J, Kathiravan K, Rajendiran N (2011) Facile synthesis of bile salt encapsulated gold nanoparticles and its use in colorimetric detection of DNA. *J Phys Chem C* 115(15266):15273
23. Sharp PA, Sugden B, Sambrook J (1973) Detection of two restriction endonuclease activities in *Haemophilus parainfluenzae* using analytical agarose-ethidium bromide electrophoresis. *Biochemistry* 12(3055):3063
24. Sambrook J, Russell DW (2001) *Molecular cloning: a laboratory manual*, vol 1, 3rd edn. Cold Spring Harbor Laboratory Press, New York, p 1.150
25. Aaij C, Borst P (1972) The gel electrophoresis of DNA. *Biochim Biophys Acta* 269(192):200
26. Mullis KB, Faloona FA (1987) Specific synthesis of DNA in-vitro via a polymerase catalyzed chain reaction. *Methods Enzymol* 155(335):350
27. Telenius H, Carter NP, Bebb CE, Nordenskjold M, Ponder BAJ, Tunnacliffe A (1992) Degenerate oligonucleotide primed PCR: general amplification of target DNA by a single degenerate primer. *Genomics* 13(718):725
28. Alonso A, Almendral MJ, Curto Y, Criado JJ, Rodri'guez E, Manzano JL (2006) Determination of the DNA-binding characteristics of ethidium bromide, proflavine, and cisplatin by flow injection analysis: usefulness in studies on antitumor drugs. *Anal Biochem* 355(157):164
29. Muniyappa V, Venkatesh HM, Ramapp HK, Kulkarni RS, Zeidan M, Tarba C-Y, Ghanim M, Czosnek H (2000) Tomato leaf curl virus from bangalore (ToLCV- an4): sequence comparison with indian ToLCV isolates, detection in plants and insects, and vector relationships. *Arch Virol* 145(1583):1598
30. Waring MJ (1965) Complex formation between ethidium bromide and nucleic acids (1965). *J Mol Biol* 13(269):282
31. Lepecq J-B, Paoletti C (1967) A fluorescent complex between ethidium bromide and nucleic acids. Physical-chemical characterization. *J Mol Biol* 27(87):106
32. Vardevanyan PO, Antonyan AP, Parsadanyan MA, Davtyan HG, Karapetyan AT (2003) The binding of ethidium bromide with DNA: interaction with single and double-stranded structures. *Exp Mol Med* 35(527):533
33. Ganguli M, Venkatesh Babu J, Maiti S (2004) Complex formation between cationically modified gold nanoparticles and DNA: an atomic force microscopic study. *Langmuir* 20(5165):5170
34. Liu J (2012) Adsorption of DNA onto gold nanoparticles and graphene oxide: surface science and applications. *Phys Chem Chem Phys* 14(10485):10496
35. Gao D, Sheng Z, Han H (2011) An ultrasensitive method for the detection of gene fragment from transgenics using label-free gold nanoparticle probe and dynamic light scattering. *Anal Chim Acta* 696(1):5